

# The Influence of *P. fluorescens* Cell Morphology on the Lytic Performance and Production of Phage φIBB-PF7A

Sanna Sillankorva · Diana Pires · Hugo Oliveira ·  
Peter Neubauer · Joana Azeredo

Received: 14 April 2011 / Accepted: 12 July 2011 / Published online: 26 July 2011  
© Springer Science+Business Media, LLC 2011

**Abstract** This study aims at assessing the influence of *Pseudomonas fluorescens* cell morphology on the effectiveness and production of the lytic bacteriophage φIBB-PF7A. *P. fluorescens* were cultured as rods or as elongated cells by varying the temperature and rotary agitation conditions. Cells presented rod shape when grown at temperatures up to 25°C and also at 30°C under static conditions, and elongated morphology only at 30°C when cultures were grown under agitation. Elongated cells were 0.4 up to 27.9 μm longer than rod cells. Rod-shaped hosts were best infected by phages at 25°C which resulted in an 82% cell density reduction. Phage infection of elongated cells was successful, and the cell density reductions achieved was statistically similar ( $P > 0.05$ ) to those obtained at the optimum growth temperature of *P. fluorescens*. Phage burst size varied with the cell growth conditions and was approximately 58 and 153 PFU per infected rod and elongated cells, grown at 160 rpm, at 25°C (the optimal

temperature) and 30°C, respectively. Phage adsorption was faster to elongated cells, most likely due to the longer length of the host. The surface composition of rod and elongated cells is similar in terms of outer membrane proteins and lipopolysaccharide profiles. The results of this study suggest that the change of rod cells to an elongated morphology does not prevent cells from being attacked by phages and also does not impair the phage infection.

## Introduction

A bacterial genus presents typically one or a limited subset of different morphologies within the forms rods, variations of rods, or cocci. Cells can change their shape in response to adverse environments (for example, nutrient limitation) or during the course of pathogenesis which might improve their survival chances. It is suggested that the variability of shapes is greatly due to bacterial defense mechanisms against adverse conditions and predation. Bacterial morphology can aid bacteria against predation by allowing them: (i) to escape by being too small or too fast, (ii) to resist ingestion by becoming too large or too long, and (iii) to become inaccessible by growing in aggregates or biofilms [29]. Moreover, cell morphology can also have a role in optimizing cell attachment to surfaces, passive dispersal, active motility, and internal or external differentiation [28].

Bacteriophages (phages) are bacterial viruses discovered nearly 100 years ago. Since then, a vast amount of research has been carried out with different phage-host systems and it is commonly accepted that the effectiveness of bacteriophages in lysing their hosts depends greatly on the target bacterium but also on external factors which can highly influence phage growth parameters.

S. Sillankorva (✉) · D. Pires · H. Oliveira · J. Azeredo  
IBB - Institute for Biotechnology and Bioengineering,  
Centre of Biological Engineering, Universidade do Minho,  
Campus de Gualtar, 4710-057 Braga, Portugal  
e-mail: s.sillankorva@deb.uminho.pt

S. Sillankorva  
Bioprocess Engineering Laboratory, Department of Process  
and Environmental Engineering and Biocenter Oulu,  
University of Oulu, P.O. Box 4300, Oulu, Finland

P. Neubauer  
Department of Biotechnology, Technische Universität Berlin,  
Berlin, Germany

In a recent work, biofilms of *Pseudomonas fluorescens*, a psychrotrophic bacterium, were observed to acquire rod and elongated shapes depending on the conditions used [21] which were both infected by phage φIBB-PF7A. However, the influence of infection of these different morphologies on progeny phage production remained unclear. Thus, this study aims at understanding the impact of cell morphology on the level of outer membrane proteins (OMP) and lipopolysaccharides (LPS) (possible phage receptors), and evaluating the influence of *P. fluorescens* cell morphology on phage adsorption and production.

## Materials and Methods

### Bacteria and Bacteriophage

*Pseudomonas fluorescens* PF7A was previously selected and used to isolate bacteriophage φIBB-PF7A [20]. The bacterium was grown at 30°C in Tryptic Soy Broth or in solid TSA medium with 1.2 % wt/vol of agar. Bacteriophage φIBB-PF7A was propagated using the double soft agar layer described by Sambrook and Russell [19].

### Phage Titration

Bacteriophage φIBB-PF7A titers were determined using the double agar layer described by Adams [1].

### Effect of Different Parameters on Cells

*Pseudomonas fluorescens* were grown in TSB at different temperatures (5, 10, 15, 20, 25, and 30°C) and rotational agitation speeds (no speed, 160, and 200 rpm) until mid-exponential phase (OD 0.8–0.9). After growth, cultures were centrifuged ( $9,000 \times g$ , 10 min, 4°C), and the pellet was resuspended in spent media (supernatant of the respective growth condition) and adjusted to an optical density at 600 nm (OD<sub>600</sub>) of 1.0. The OD<sub>600</sub> values were transformed to numbers of viable cells (CFU ml<sup>-1</sup>) through calibration curves made with cells presenting rod shape and elongated morphology. The resulting equations are as follow: nr rod cells (CFU ml<sup>-1</sup>) =  $1.70 \times 10^9 \times OD_{600} + 2.77 \times 10^9$ ; nr elongated cells (30°C, 160 rpm) (CFU ml<sup>-1</sup>) =  $6.45 \times 10^8 \times OD_{600} + 6.60 \times 10^6$ ; and nr elongated cells (30°C, 200 rpm) (CFU ml<sup>-1</sup>) =  $3.72 \times 10^7 \times OD_{600} + 1.75 \times 10^5$ . Viable cell counts were determined and an OD<sub>600</sub> of 1.0 of cultures grown at 30°C using rotary agitations of 160 and 200 rpm correspond to  $5.90 \times 10^8$  and  $3.80 \times 10^7$  cells ml<sup>-1</sup>, respectively. In cultures grown from 5 to 25°C and at 30°C under static conditions, this OD<sub>600</sub> corresponds to  $7.60 \times 10^9$  cells ml<sup>-1</sup>, respectively.

### Phage Infection of *P. fluorescens* Cells

125 µl of *P. fluorescens* cultures (OD<sub>600</sub> 1.0) and 125 µl of a phage in SM buffer (5.8 g l<sup>-1</sup> NaCl, 2 g l<sup>-1</sup> MgSO<sub>4</sub>·7H<sub>2</sub>O, 50 ml l<sup>-1</sup> 1 M TRIS, pH 7.5), at a concentration to give a multiplicity of infection (MOI) of 0.15, were placed in 96-well microplates. The control corresponds to 125 µl of bacterial suspension and 125 µl of SM buffer. Infection experiments were followed through OD<sub>600</sub> measurements and determination of phage titer. Three independent experiments were performed.

### Phage One-Step Growth and Adsorption Experiments

One-step growth curves and adsorption assays were performed at room temperature as described by Sillankorva et al. [20, 21].

### Field Emission Scanning Electron Microscopy (FESEM)

Cell suspensions were placed on stainless steel slides and fixed with 2.5% (v/v) glutaraldehyde (4°C, 1 h). After, samples were washed by immersion in PBS, dehydrated in ethanol, and critical point dried (Critical Point Dryer CPD 030). Samples were coated with platinum and analyzed with Field Emission Scanning Electron Microscopy (FESEM) (JEOL JSM-6300F instrument).

### Outer Membrane Protein Isolation and Analysis

Outer membrane proteins (OMP) were isolated according to the method described by Masuda et al. [15]. OMPs were separated by sodium dodecyl sulfate polyacrylamide gel electrophoresis (SDS-PAGE) [11] (12% (wt/vol)) acrylamide, at a constant current of 14 mA, and after that gels were silver stained.

### Lipopolysaccharide Extraction

Lipopolysaccharides (LPS) were extracted using the LPS extraction kit (iNtRON) according to the manufacturer's instructions. LPS were separated using an urea-based SDS-PAGE as described by Maskell [14]. For this, 10% (wt/vol) acrylamide gels containing 2.88 g of urea were run at a constant current of 14 mA. After, the gels were silver stained.

### Statistical Analysis

To compare the cell density reductions after the different phage experiments performed, analysis of variance

(ANOVA single factor from MS Office) was used. In all the analysis performed, the confidence interval used was 95%.

## Results

### Effect of Temperature on Cell Length and Phage Infection

To evaluate morphological alterations, planktonic *P. fluorescens* cells grown at 160 rpm and at different temperatures were analyzed by FESEM. The bacterium presented rod shape (Fig. 1a) when grown in the range of 5–25°C and elongated shape when grown at 30°C (Fig. 1b). The length of rod cells was in average 2.38 µm and the minimum length of elongated cells was 4.2 µm and grew up to a maximum cell length of 23.8 µm (Table 1).

In experiments carried without phage (controls), the cells continued to grow (Fig. 1c) while cell density of phage infected planktonic cultures decreased (Fig. 1d). Lysis of rod cells was enhanced and statistically different ( $P < 0.05$ ) at 25°C (Fig. 1d) compared to all other

temperatures which produced rod-shaped cells (5–20°C). At this temperature, phages caused an approximately 82% of cell density reduction compared to control samples (Table 1). Cell density reduction (80%) of phage infection of elongated cells, grown at 30°C, was not significantly different ( $P > 0.05$ ) from cells infected at 25°C (Table 1). Phage replication inside cells with reduced specific growth rate (5 and 10°C) (Table 1), led to low numbers of progeny phages produced (Fig. 1e).

One-step growth experiments performed at room temperature (RT) showed that the latent and rise periods were not influenced by cell morphology; however, the burst size varied considerably resulting, after 60 min, in approximately 58 (rod) and 150 (elongated) progeny phages per infected cells (Fig. 2a). Furthermore, adsorption assays, also performed at RT, showed a slightly faster adsorption of phages to elongated cells (Fig. 2b). The adsorption rates for rod and elongated cells, calculated according to Barry and Walter [2], were of  $3.97 \times 10^{-10}$  and  $4.21 \times 10^{-10}$  ml min $^{-1}$  for a period of 4 min, respectively.

The *P. fluorescens* OMP and LPS profiles remained similar regardless of cell morphology (Fig. 2c, d).

**Fig. 1** Morphology and infection of *P. fluorescens* cells grown at 160 rpm at different temperatures. **a** Morphology of cells grown at 5°C and **b** 30°C, **c** cell density of control samples and **d** after phage infection of cells at different temperatures using a MOI of 0.15, and **e** phage concentration at different time periods. Error bars shown indicate standard deviations of three parallel 96-well plates analyzed and the error bars in phage numbers indicate standard deviations from three independent experiments

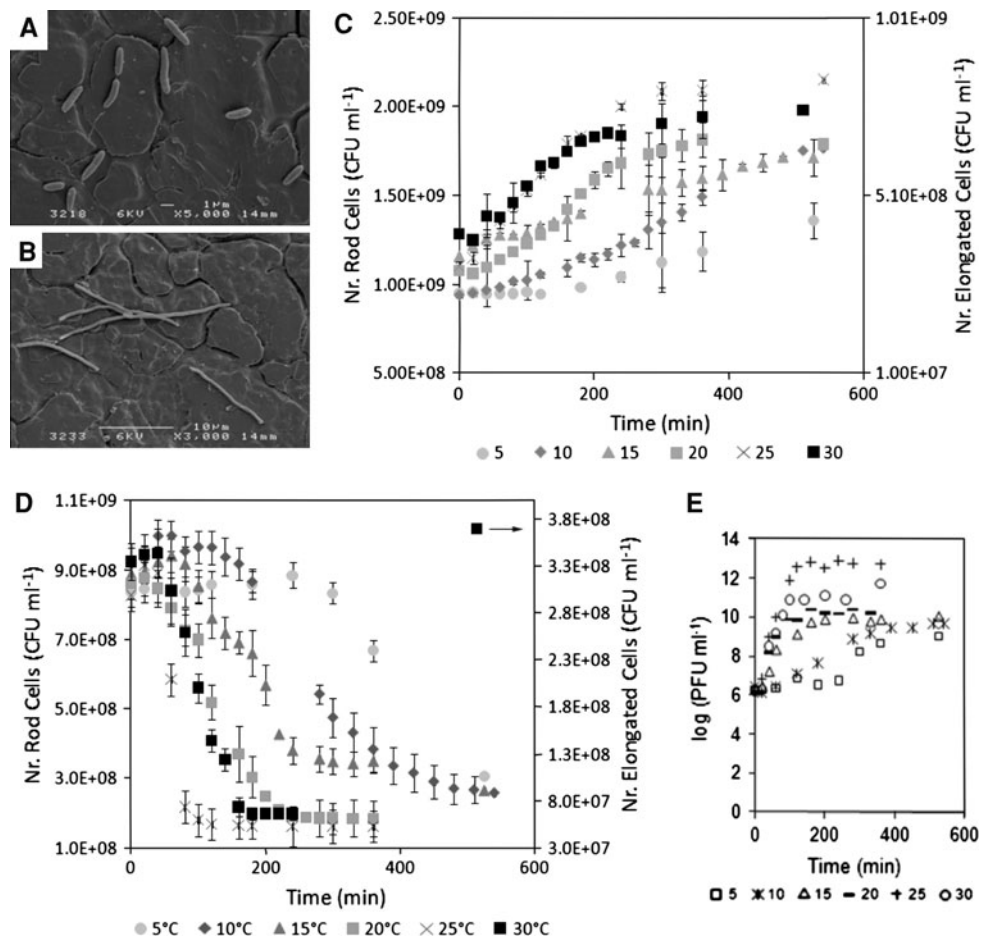


**Table 1** Influence of temperature and rotational agitation speed on *P. fluorescens* PF7A cell length, specific growth rate, cell number at an OD<sub>600</sub> of 1, and cell density decrease (%) after phage infection using a MOI of 0.15

T (°C), Speed (rpm)	Cell length <sup>a</sup> (μm) (±SD) [min (μm)–max (μm)] <sup>b</sup>	μ (h <sup>-1</sup> ) (±SD)	Log (CFU ml <sup>-1</sup> )	OD <sub>600</sub> decrease (%) (±SD)
5, 160	2.14 (0.84) [1.6–3.6]	0.025 (0.001)	9.85 (0.03)	67.80 (3.08)
10, 160	2.28 (0.87) [1.7–3.7]	0.047 (0.002)	9.89 (0.02)	69.33 (2.75)
15, 160	2.25 (0.90) [1.7–3.8]	0.070 (0.004)	9.85 (0.04)	61.54 (4.05)
20, 160	2.54 (0.43) [2.3–3.3]	0.087 (0.004)	9.86 (0.05)	73.08 (3.75)
25, 160	2.70 (0.45) [2.4–3.4]	0.122 (0.003)	9.88 (0.04)	82.37 (1.94)
30, 160	14.80 (7.30) [4.2–23.8]	0.084 (0.003)	8.77 (0.12)	79.75 (6.75)
30, 0	2.04 (0.78) [1.5–3.3]	0.048 (0.004)	9.88 (0.04)	27.04 (4.50)
30, 160	14.80 (7.30) [4.2–23.8]	0.084 (0.003)	8.77 (0.12)	79.75 (6.75)
30, 200	20.7 (7.12) [11.3–29.2]	0.127 (0.002)	7.58 (0.04)	84.15 (2.38)

SD standard deviations

<sup>a</sup> Minimum and maximum size from measurements of 5–10 cells

<sup>b</sup> Minimum and Maximum cell length observed

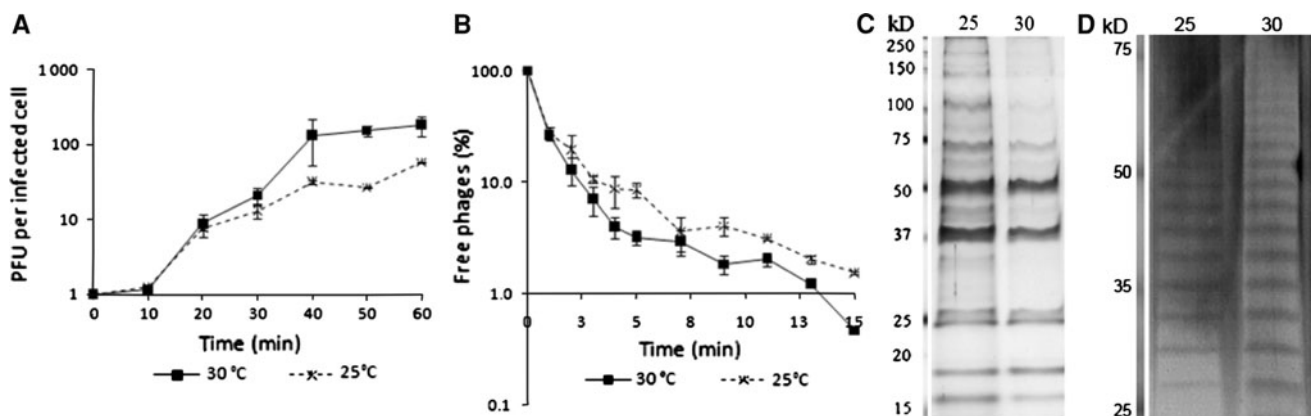


**Fig. 2** Phage φIBB-PF7A **a** one-step and **b** adsorption experiments to *P. fluorescens* grown at 25 and 30°C where error bars indicate standard deviations of three independent experiments, **c** the outer membrane protein profiles and **d** LPS of cells grown at 25 and 30°C,

respectively. Precision Plus Protein All Blue standard (Bio-Rad) and Protometrics (National Diagnostics) were the protein standards used in the SDS-PAGE and LPS gels, respectively

#### Effect of Rotational Agitation at 30°C on Cell Length and Phage Infection

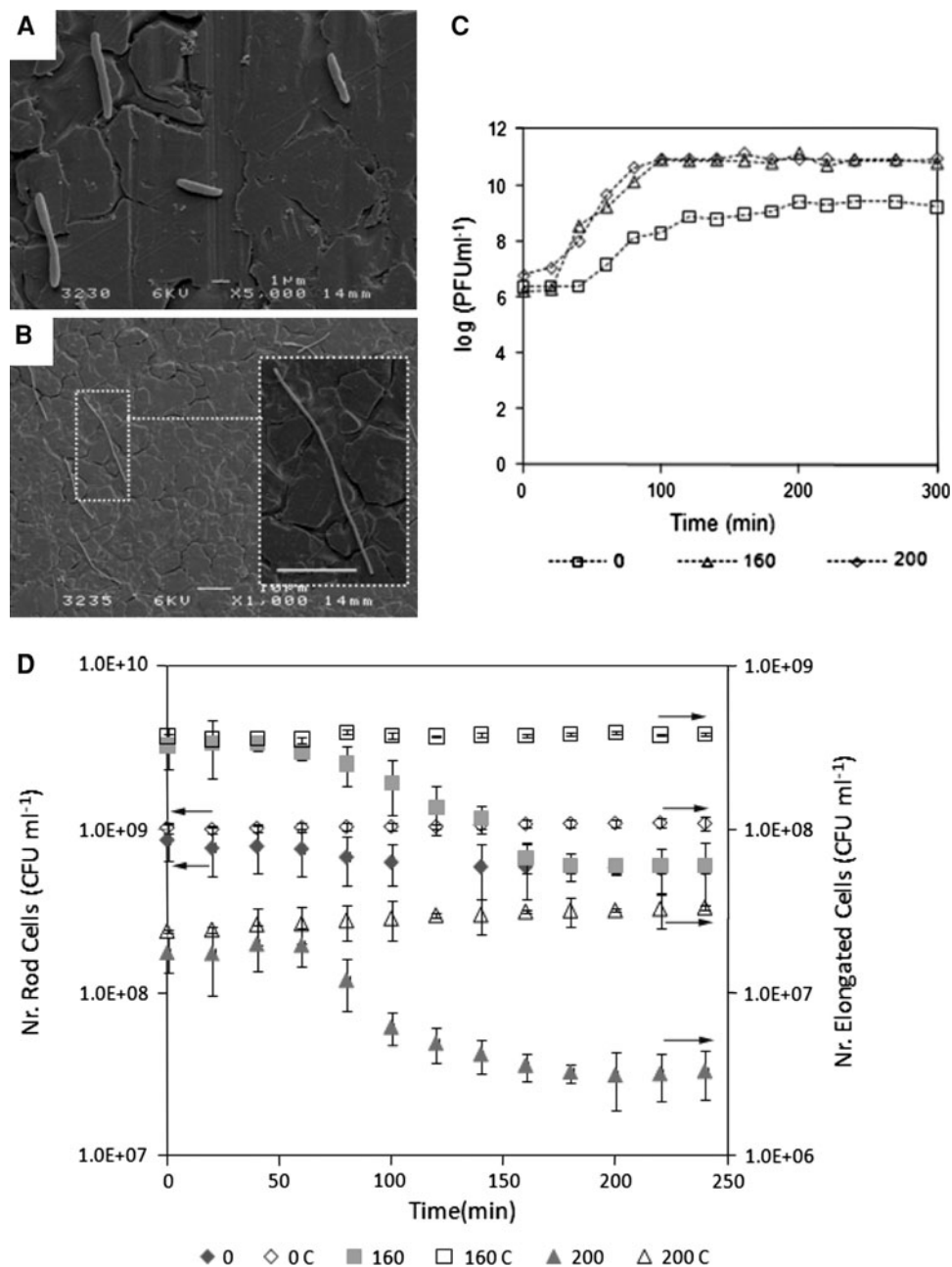
Morphology of planktonic cultures grown at 30°C varying the rotational agitation (0, 160, and 200 rpm) and the efficacy of phage infection at these different conditions were investigated. At 30°C, cells grown under static conditions (0 rpm) continued to have typical rod morphology (Fig. 3a) with a length of 2.04 μm. Under agitation, cell length increased and varied greatly (see minimum and maximum lengths in Table 1) but cell width remained similar to that observed in rod cells. At the maximum speed studied (200 rpm), the longest cell lengths observed was 29.2 μm (Fig. 3b; Table 1). The growth rate (h<sup>-1</sup>) of the bacterium varied with the speed being approximately 2.6 times slower at 0 rpm than at 200 rpm (Table 1). Despite

the difference in the initial numbers of elongated cells produced at 160 and 200 rpm, the infection using a MOI of 0.15 resulted in similar lysis profiles (Fig. 3d) and not in statistically different cell density reductions ( $P > 0.05$ ). Also the increase of phage numbers at these two conditions was similar (Fig. 3c). Phage infection at 0 rpm was significantly different ( $P < 0.05$ ) from infection under agitated conditions, and overall was not efficient resulting in a very low decrease of cell density (30%) (Table 1), and in a low increase of phage titer (Fig. 3d).

#### Discussion

In previous studies, we have demonstrated that phage killing efficacy of *P. fluorescens* cells is greatly dependent

**Fig. 3** Morphology and infection of *P. fluorescens* cells grown at 30°C under varied shake speeds. **a** Morphology of cells grown at 0 rpm and **b** 200 rpm, **c** phage concentration at different time periods and **d** cell density of control samples and of samples after phage infection of cells at different shake speeds using a MOI of 0.15



on the bacterial growth conditions. We further noticed that in biofilms this bacterium exhibits different morphologies (rod and elongated) upon different growth conditions which may affect the phage infection process. In order to disclose the effect of cell size and morphology in phage infection, two factors influencing *P. fluorescens* morphology were used to trigger changes in the morphology and physiology of planktonic cells which were further infected with phages. This particular *P. fluorescens* strain becomes filamentous at a growth temperature of 30°C but combined with the existence of agitation, since under non-agitated

conditions at 30°C the cells maintain a rod shape. Rod-shaped *P. fluorescens* cells were produced at temperatures between 5 and 25°C and at 30°C under static conditions, and their lengths varied between 1.5 and 3.8 μm. The length of filamentous cells varied between minimum and maximum lengths of 4.2 and 29.2 μm. This filamentous morphology is most likely due to a blocking of the cell division process as described for *Pseudomonas aeruginosa* and *Escherichia coli* [7, 12, 17, 23–26] resulting from one or more proteins required in cell division which become nonfunctional. Furthermore, several studies report that

blocking of cell division does not affect cell growth including parameters such as: growth rate, DNA replication, and chromosome segregation [6, 13, 18].

Overall, phage efficacy did not specifically depend on the cell length since elongated cells were as efficiently lysed as rod-shaped cells. Despite the similarities in phage efficacy observed in optimally growing rod cells and elongated cells, we analyzed the production of phages inside these morphologically distinct cells. Phage one-step growth curve results showed that elongated cells were capable of producing three times more progeny phages than rod hosts grown at the optimal temperature and with a 1.45-fold faster specific growth rate. Nevertheless, the latency period and raise period were not influenced by cell size. In addition, the adsorption rate of elongated cells was only slightly higher than rod shape cells. In fact, Edgar et al. [5] have suggested that phages have evolved mechanisms to utilize the asymmetry that is present in Gram-negative by preferentially adsorbing, injecting, and replicating their DNA at the bacterial poles and thus morphology seems not to play a major role in the phage infection process [5]. Distinct reports have associated bacterial filamentation caused by exposure to antibiotics with an increase in the burst size [4, 8, 10] and have showed that the burst size increases in parallel with DNA content but not with DNA concentration. According to the authors of these studies, it is the cell size rather than metabolic rate that influences the phage development in the presence of antibiotics. Nevertheless, other authors suggest that phage development depends in fact of the concentration of various resources (for example: intracellular levels of genomic DNA, RNA polymerase, ribosomes, nucleoside triphosphates, amino acids [3]) which are increased in cells with greater volumes [27]. It was surprising to observe that cells with up to 10 times longer lengths resulted only in three, and not in 10, times more progeny phages released. According to You et al. [27], a decrease in the gp10A concentration of phage T7 can be responsible for a major decrease in the procapsid assembly rate which consequently leads to a reduced number of phages produced inside of cells with large cell volumes. In a previous study performed with *P. fluorescens* biofilms and with the same phage used in this study, the phage proved to be highly efficient under static conditions leading to approximately 3 log reduction up to 5 log reduction in the amount of viable cells from biofilms of 24 h up to 5 days old biofilms after 4 h of infection, respectively [21, 22]. Thus we were expecting to achieve the same levels of efficiency in planktonic cultures, however, planktonic *P. fluorescens* cells under static conditions (0 rpm) were unexpectedly inefficient. Possibly, in static infection of planktonic cells, the efficiency of collision between phages and their hosts is reduced [9] compared to infection, under static conditions,

of biofilms cells which are found in the proximity of neighboring cells which enhances phage-host encounter.

As phages need to interact with molecules or structures, such as LPS or proteins and flagella or capsules that exist on the bacterial surface [16], so that infection can take place, we analyzed the OMP and LPS profiles of *P. fluorescens* grown of rod (25°C) and elongated cells (30°C), and found no significant differences in number of bands. Therefore, the phage receptors on the bacterial surface of rods and elongated cells are most likely to be present since otherwise the infection would have not taken place.

Phage φIBB-PF7A was efficient in killing both elongated and rod-shaped cells, and clearly a change of morphology is not, in this case, sufficient for the bacterium to evade from lysis by this specific phage. This is a clearly important fact in phage application to real environments since there cells occasionally adopt other and more uncommon morphologies.

**Acknowledgments** This work was supported by a grant (SFRH/BD/18485/2004) from the Portuguese Foundation for Science and Technology (FCT).

## References

1. Adams MH (1959) Bacteriophages. Interscience Publishers, New York
2. Barry G, Goebel W (1951) The effect of chemical and physical agents on the phage receptor of phase-II *Shigella sonnei*. J Exp Med 94:387–400
3. Bremer H, Dennis PP (1996) Modulation of chemical composition and other parameters of the cell by growth rate. In: Neidhardt FC, Curtiss R III, Ingraham JL, Lin ECC, Low KB, Magasanik B, Reznikoff WS, Riley M, Schaechter M, Umbarger HE (eds) *Escherichia coli and Salmonella: cellular and molecular biology*. American Society for Microbiology, Washington, DC, pp 1553–1569
4. Comeau AM, Tetart F, Trojet SN, Prere M-F, Krisch HM (2007) Phage-antibiotic synergy (PAS): B-lactam and quinolone antibiotics stimulate virulent phage growth. PLoS ONE 2:e799
5. Edgar R, Rokney A, Feeney M, Semsey S, Kessel M, Goldberg MB, Adhya S, Oppenheim AB (2008) Bacteriophage infection is targeted to cellular poles. Mol Microbiol 68:1107–1116
6. Errington J, Daniel RA, Scheffers DJ (2003) Cytokinesis in bacteria. Mol Biol Rev 67:52–65
7. Greenwood D, O'Grady F (1973) Comparison of the response of *Escherichia coli* and *Proteus mirabilis* to seven b-lactam antibiotics. J Infect Dis 128:1231–1240
8. Hadas H, Einav M, Fishov I, Zaritsky A (1997) Bacteriophage T4 development depends on the physiology of its host *Escherichia coli*. Microbiology 143:179–185
9. Kasman L, Kasman A, Westwater C, Dolan J, Schmidt M, Norris J (2002) Overcoming the phage replication threshold: a mathematical model with implications for phage therapy. J Virol 76:557–5564
10. Krueger AP, Cohn T, Smith PN, McGuire CD (1948) Observations on the effect of penicillin on the reaction between phage and staphylococci. J Gen Physiol 31:477–488
11. Laemmli UK (1970) Cleavage of structural proteins during the assembly of the head of bacteriophage T4. Nature 227:680–685

12. Maki N, Gestwicki JE, Lake EM, Kiessling LL, Adler J (2000) Motility and chemotaxis of filamentous cells of *Escherichia coli*. *J Bacteriol* 182:4337–4342
13. Margolin W (2000) Themes and variations in prokaryotic cell division. *FEMS Microbiol Rev* 24:531–548
14. Maskell JP (1991) The resolution of bacteroides lipopolysaccharides by polyacrylamide-gel electrophoresis. *J Med Microbiol* 34:253–257
15. Masuda N, Sakagawa E, Ohya S (1995) Outer membrane proteins responsible for multiple drug resistance in *Pseudomonas aeruginosa*. *Antimicrob Agents Chemother* 39:645–649
16. Puig A, Araujo R, Jofre J, Frias-Lopez J (2001) Identification of cell wall proteins of *Bacteroides fragilis* to which bacteriophage B40-8 binds specifically. *Microbiology* 147:281–288
17. Rolinson GN (1980) Effect of b-lacta antibiotics on bacterial cell growth rate. *J Gen Microbiol* 120:317–323
18. Rothfield LS, Justice S, Garcia-Lara J (1999) Bacterial cell division. *Annu Rev Genet* 33:423–448
19. Sambrook J, Russell DW (2001) Molecular cloning: a laboratory manual. Cold Spring Harbor Laboratory Press, Cold Spring Harbor, NY
20. Sillankorva S, Neubauer P, Azeredo J (2008) Isolation and characterization of a T7-like lytic phage for *Pseudomonas fluorescens*. *BMC Biotechnol* 8:80
21. Sillankorva S, Neubauer P, Azeredo J (2008) *Pseudomonas fluorescens* biofilms subjected to phage phiIBB-PF7A. *BMC Biotechnol* 8:79
22. Sillankorva S, Neubauer P, Azeredo J (2010) Phage control of dual species biofilms of *Pseudomonas fluorescens* and *Staphylococcus lentus*. *Biofouling* 26:567–575
23. Steinberger RE, Allen AR, Hansa HG, Holden PA (2002) Elongation correlates with nutrient deprivation in *Pseudomonas aeruginosa*—unsaturated biofilms. *Microbiol Ecol* 43:416–423
24. Werner E, Roe F, Bugnicourt A, Franklin MJ, Heydorn A, Molin S, Pitts B, Stewart PS (2004) Stratified growth in *Pseudomonas aeruginosa* biofilms. *Appl Environ Microbiol* 70:6188–6198
25. Wright JB, Costerton JW, McCoy WF (1988) Filamentous growth of *Pseudomonas aeruginosa*. *J Ind Microbiol* 3:139–146
26. Yokochi T, Narita K, Morikawa A, Takahashi K, Kato Y, Sugiyama T, Koide N, Kawai M, Fukada M, Yoshida T (2000) Morphological change in *Pseudomonas aeruginosa* following antibiotic treatment of experimental infection in ice and its relation to susceptibility to phagocytosis and to release of endotoxin. *Antimicrob Agents Chemother* 44:205–206
27. You LC, Suthers PF, Yin J (2002) Effects of *Escherichia coli* physiology on growth of phage T7 in vivo and in silico. *J Bacteriol* 184:1888–1894
28. Young KD (2006) The selective value of bacterial shape. *Microbiol Mol Biol Rev* 70:660–703
29. Young KD (2007) Bacterial morphology: why have different shapes? *Curr Opin Microbiol* 10:596–600